

DIPOLE MODELING IN FASTICA DECOMPOSITION OF EVOKED RESPONSES

Ricardo Nuno Vigário

Neural Network Research Centre
Helsinki University of Technology
P.O. Box 5400, FIN-02015 HUT, Finland
Ricardo.Vigario@hut.fi

ABSTRACT

When applied to the decomposition of evoked responses, independent component analysis (ICA) is often used in a blind source separation framework, i.e., the goal is to identify underlying source signals from their instantaneous linear mixtures, with no prior knowledge on the sources or the mixing process. Yet, often some modeling is explicitly or implicitly added when attempting to give a physiologically plausible interpretation to the result of the decomposition.

Here we assume that all the relevant independent components can be modeled using equivalent current dipoles (ECDs). The incorporation of this modeling information should simplify the search for the underlying brain activated sources, while giving better physiological grounds to ulterior interpretations of the decomposed signals.

1. INTRODUCTION

Over the past years, we have observed [7, 8] the suitability of ICA approaches to analyze several types of neuromagnetic evoked responses. In particular, we showed that ICA differentiates well between somatosensory and auditory brain responses in the case of a combined vibrotactile stimulation. Furthermore, the independent components, found with no other modeling assumption than their statistical independence, exhibit field patterns that agree with the conventional current dipole models.

The study presented in this paper consists of a modification on an existing ICA algorithm, in order to add an explicit stage of dipolar modeling into the search for the independent components. This new iterative method is applied to the decomposition of somatosensory and auditory evoked fields.

2. THE ALGORITHMS

As in most ICA formulations, we will assume that our averaged magnetoencephalographic evoked responses consist of instantaneous linear mixtures of underlying independent source signals, under the noise free model:

$$\mathbf{x}_k = \mathbf{A}\mathbf{s}_k,$$

where \mathbf{x}_k is an L -dimensional measuring vector, made up of the L mixtures at discrete time k . \mathbf{s}_k is the M -dimensional vector with the independent source signals ($M \leq L$), and \mathbf{A} is the instantaneous linear mixing matrix. Both \mathbf{s}_k and \mathbf{A} are the unknowns we wish to identify. The first corresponds to the time activations of the brain regions involved in the evoked responses. The columns of the second are the field patterns mapping those signals to the measurements.

2.1. The original FastICA

At the basis of the present research, we use the FastICA algorithm, which was introduced in [3]. It is a fixed point algorithm that finds the independent signals through the maximization of the absolute value of their kurtosis. The measured data is previously whitened ($\mathbf{v} = \mathbf{\Lambda}^{-1/2}\mathbf{\Xi}^T\mathbf{x}$, where $\mathbf{\Lambda}$ is a diagonal matrix with the eigenvalues of the data covariance matrix $E\{\mathbf{x}\mathbf{x}^T\}$, and $\mathbf{\Xi}$ a matrix with the corresponding eigenvectors as its columns). A compression is often performed during the whitening, in order to prevent overlearning related artifacts (“bumpy” signals are typically visible when using poor compression rates [4]). Each l th iteration to find the separation vector \mathbf{w} is then defined as

$$\begin{aligned}\mathbf{w}^*_l &= E\{\mathbf{v}(\mathbf{w}_{l-1}^T\mathbf{v})^3\} - 3\mathbf{w}_{l-1} \\ \mathbf{w}_l &= \mathbf{w}^*_l / \|\mathbf{w}^*_l\|.\end{aligned}\tag{1}$$

FastICA can be used both in a symmetrical and a deflationary manner. If the independence is not fully

guaranteed, the error of assuming it will be somewhat spread to all ICs in the symmetrical version. In the deflationary, the early components are more likely to fit the criterion, as the later ones will have to deal with accumulated errors from the previous components.

In the present work, FastICA will be used in its deflationary version, to extract one single component. The independence of this component should then be the most reliable one. Yet, the order of appearance of the ICs is undetermined in ICA, therefore different initial conditions can lead to different first guesses from the algorithm. Due to the very fast convergence of the FastICA, as much as 100 different initial conditions were tested, and their results gathered. Only a few different signals were consistently picked using this method, as can be seen in Fig. 2.

2.2. Adding dipole modeling to FastICA

As stated above, dipole modeling is often assumed when validating the ICs and locating the corresponding neural sources. In fact, often the field patterns, mapping the components to the measurements, fit well the dipole modeling assumptions. Note that the field patterns correspond to the columns of the mixing matrix \mathbf{A} .

In order to extract more than one independent component, we have to insure that the contributions of the ones already found are extracted from the original data. This can be done by explicit subtraction of the IC, or by imposing the orthogonality of the spaces defined by successive components.

We now propose to remove, not the independent component itself, but the magnetic field produced by one or more equivalent current dipoles (ECDs) that fit the best the respective IC. With this change, the independence criterion is somewhat relaxed, but with an increase in the explanation power of the resulting component. This modified or iterated FastICA algorithm is therefore a good compromise between pure independence and conventional ECD fitting.

All ICA runs were made using MATLAB code, based on the FastICA package [1]. All measurements and source localizations were carried out using a Neuromag-122TM system and its signal processing software.

3. STIMULI AND EXPERIMENTAL SETUP

The evoked fields used in this paper, were recorded at the Brain Research Unit of the Low Temperature Laboratory of the Helsinki University of Technology, in a magnetically shielded room, using a 122-channel whole-scalp neuromagnetometer [2]. They consisted of responses to vibrotactile stimuli, generated with a bass-reflex loudspeaker and a tube delivering the tone into

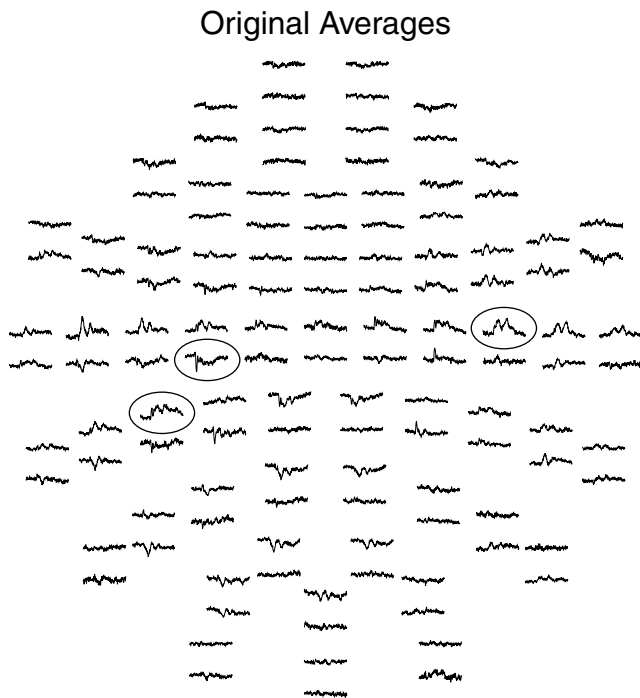


Figure 1: *Data set used – averaged responses to vibrotactile stimuli.*

the magnetic shielded room. That was coupled to a balloon which was held by the subject with both hands. Both tactile and the concomitant auditory stimuli were thus present. Further details on the stimuli and the setup can be found in [5].

Figure 1 shows the complete set of 122 averaged evoked responses. Three inserts in the figure highlight equal number of signal types present in the measurements. On the leftmost one, we can see a step-like signal. The middle one shows a sharp and early response, originated in the primary somatosensory cortex. The rightmost insert has a broader signal, with longer latency than the previous one, which is associated with the primary auditory responses.

4. RESULTS

Figure 2 shows the results of the ICA decomposition of the evoked responses. The left column has the four independent components found from 100 runs of the original FastICA on the complete data set, changing the initial conditions after each run. These results agree with the ones presented in an earlier report [8], and explain well some of the signals seen in Fig. 1: OrIC1 and OrIC3 have latencies that are characteristic of the auditory responses visible in the rightmost insert, whereas

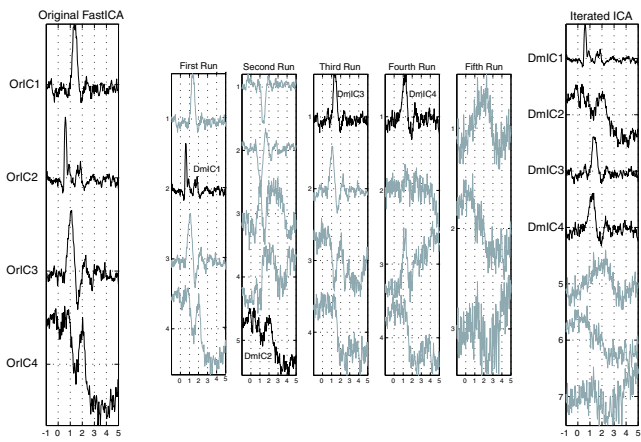


Figure 2: *ICA decomposition of the evoked responses. On the left are depicted the ICs corresponding to a single run of FastICA, whereas on the right are the ones corresponding to the modified algorithm. The middle 5 columns show the construction of the components of the right hand side.*

OrIC2 and OrIC4 are clearly related to the somatosensory and step-like inserts. The locations of the ECDs associated to these independent components are shown in Fig. 3. Once again, it is clear that they agree with the expected brain regions to be activated by the particular stimulus mode. Note that only the last component required three dipoles to correctly explain the respective IC. One of the ECDs explaining OrIC4 originates from the primary somatosensory area, already used to explain OrIC2.

The ICs shown in the right column of Fig. 2 have been produced by the modified FastICA algorithm. After each set of 100 runs of FastICA, the most frequently observed IC was kept. The magnetic field associated to its best ECD fit was then extracted from the original data. The n th independent component is now sought from a set of 122 dimensional signals, from which the ECD contributions of the previous $n - 1$ components have been removed. The 5 columns in the middle show each step of the long iterative process leading to the final set of signals on the right. Note that, on the second run, the signal picked was not the one corresponding to the auditory response, as we could have wished for, but rather the step-like one. This is due to the fact that the choosing criterion has no way to evaluate the goodness or physiological usefulness of each component.

Figure 4 shows the field patterns of the independent components found using the dipole modeled FastICA algorithm, and respective ECDs. It is clear that DmIC1 and DmIC3 present great resemblance to

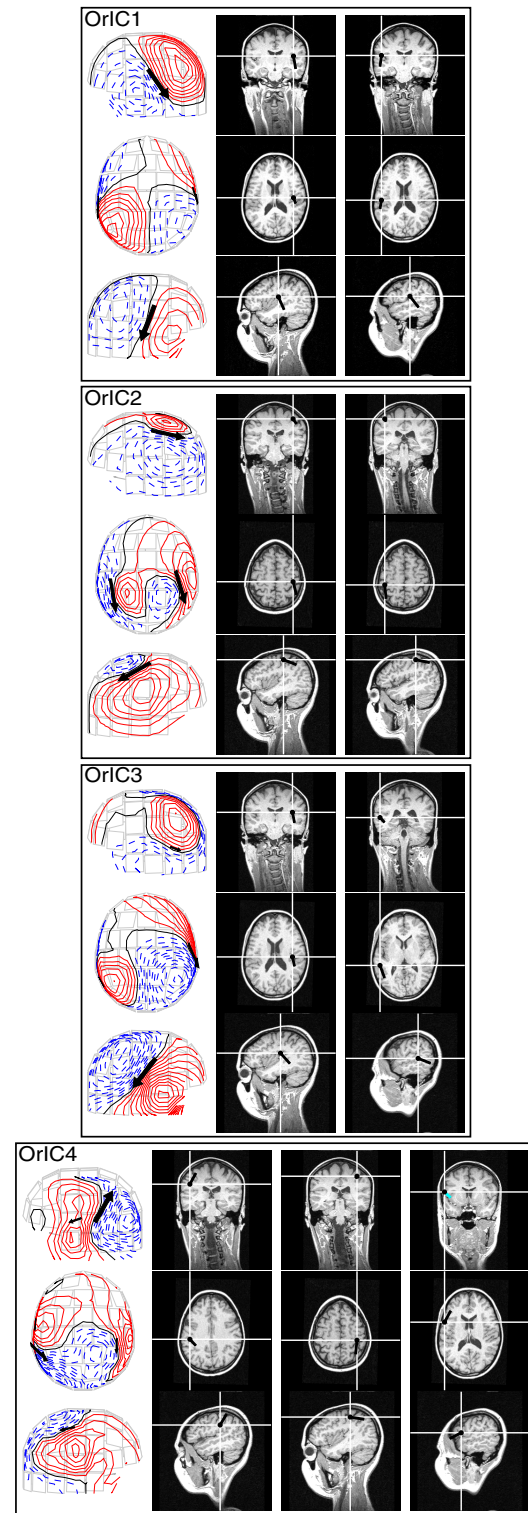


Figure 3: *Localizations of the ECDs corresponding to the "regular" FastICA decomposition.*

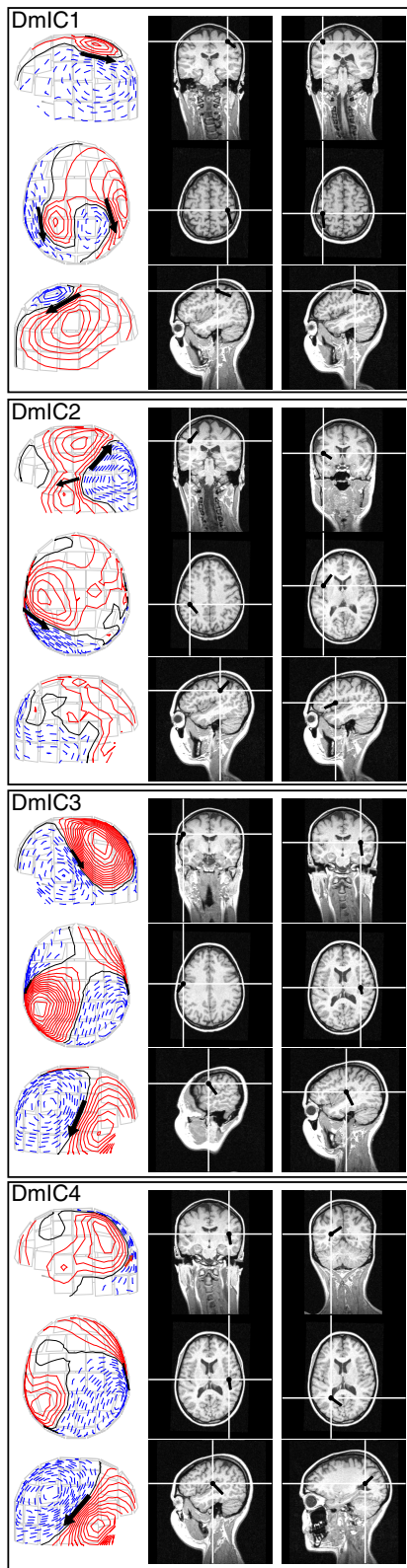


Figure 4: Localization of the “iterated” FastICA.

OrIC2 and OrICA1, the same can not be said from the other ICs. Due to an early extraction of the somatosensory ECDs, no such dipole was required to explain DmIC2, reducing here the total number of dipoles from 9 to 8. Furthermore, the pattern on the left side of DmIC2 is now much clearer than that of OrIC4. Finally, it is as well visible that DmIC4’s patterns are simpler than those of the corresponding original decomposition (OrIC3).

One measure of the ability of the modeled dipoles to explain the measured magnetic fields is given by the goodness-of-fit (gof) [6], a normalized squared error between the measurements and the fields produced by the modeled sources:

$$g = \left(1 - \frac{\sum_i (\mathbf{b}_i - \mathbf{m}_i)^2}{\sum_i \mathbf{m}_i^2} \right) \times 100\%.$$

The summations run over the complete set of sensors. The higher the g , the better the explanation. If $g = 100\%$, the model fully explains the measurements, if $g = 0\%$, it does not perform any better than a zero field fit would.

In Fig. 5 we see the gof values attained by the complete sets of ECDs associated to both ICA implementations. The solid line shows the combined performance of the 9 dipoles corresponding to the four FastICA components, whereas the dashed line shows the performance of the 8 corresponding to the iterated FastICA decomposition. It is clear that the modified ICA algorithm explains the measured data at least as well as the traditional algorithm does, with increased performance on occasions (see, e.g., the portion corresponding to the activation of the primary auditory area).

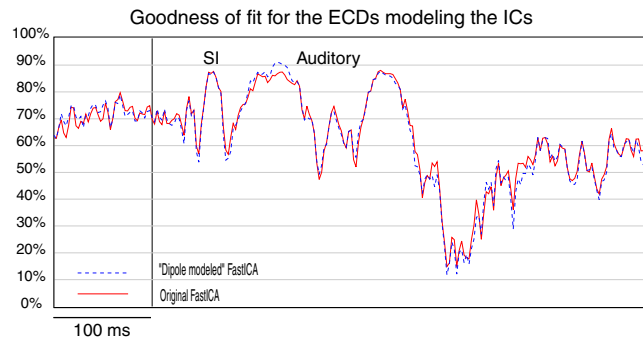
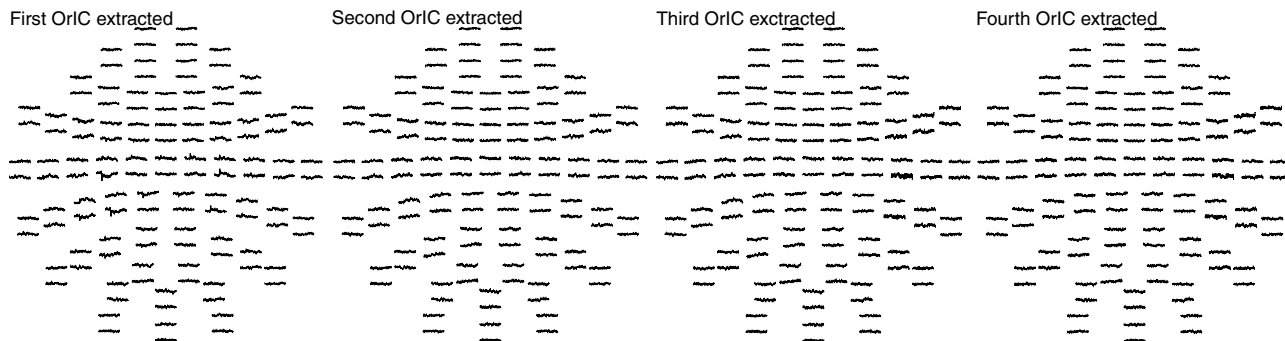


Figure 5: Goodness-of-fit for the ECDs associated with the two FastICA algorithms.

Another way to look into the different behaviors of the two algorithms, is through the analysis of the remaining measured signals, after extracting the magnetic fields originated by the ECDs corresponding to

Extraction of the ECDs corresponding to the OrICs



Extraction of the ECDs corresponding to the DmICs

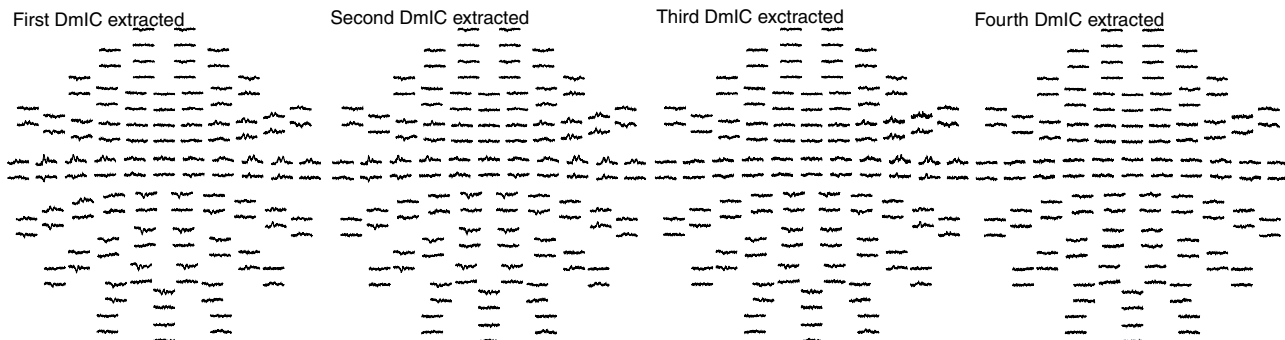


Figure 6: *Unexplained magnetic fields, after extracting each independent component's contribution.*

each independent component.

In Fig. 6, we show these remaining magnetic fields for both the conventional FastICA (top), and the modified one (bottom). On the original FastICA results, the extraction of the first IC results in the suppression of all auditory related components. Removing the second component leads to a very simplified set of remaining signals, that seems to change only after the extraction of the fourth component, in which the step-like signal disappears.

In the modified algorithm, after extracting the first IC from the original data, the somatosensory related signal is suppressed. The step-like is removed after the second. It is important to note that the extraction of the third IC doesn't result in a complete suppression of the auditory responses. In fact, the right-hand side responses are just attenuated at this stage, and removed only after the extraction of the fourth IC. This is a good indication that this algorithm is actually able to detect the lateralization effects visible when the auditory stimuli are applied mainly to one ear (see [9] for a study of pure auditory evoked responses, where this issue is dealt in detail).

5. DISCUSSION

We have used the speed and deflationary characteristics of the FastICA algorithm to derive an iterative algorithm incorporating source modeling in its search for independent decomposition of combined somatosensory and auditory evoked responses.

Globally, we may say that the modified FastICA algorithm achieved better separation abilities, while keeping the very high agreement with the physiological plausibility of its independent components. In particular, we have seen that a fewer number of equivalent current dipoles were needed to attain a better explanation of the measured recordings than when using a traditional FastICA approach.

The detection of subtle information, such as lateralization effects, were as well rendered possible with the modified algorithm which were not visible in the original FastICA formulation.

Further experiments should be carried out, in order to identify the overlaps, limitations and complementarities in the performances of each algorithmic approach. As well, at each iteration of the modified FastICA, we

have picked the most frequent component. Other criteria, that may lead to improved results, could choose the components with simpler or more dipolar field pattern instead.

6. REFERENCES

- [1] *FastICA MATLAB package*. Available at the WWW address:
<http://www.cis.hut.fi/projects/ica/fastica>.
- [2] M. Hämäläinen, R. Hari, R. Ilmoniemi, J. Knuutila, and O. V. Lounasmaa. Magnetoencephalography— theory, instrumentation, and applications to noninvasive studies of the working human brain. *Reviews of Modern Physics*, 65(2):413–497, 1993.
- [3] A. Hyvärinen and E. Oja. A fast fixed-point algorithm for independent component analysis. *Neural Computation*, 9:1483–1492, 1997.
- [4] A. Hyvärinen, J. Särelä, and R. Vigário. Spikes and bumps: artefacts generated by independent component analysis with insufficient sample size. In *Proc. Int. Workshop on Independent Component Analysis and Blind Separation of Signals (ICA '99)*, Aussois, France, 1999.
- [5] V. Jousmäki and R. Hari. Somatosensory evoked fields to large-area vibrotactile stimuli. *Clinical Neurophysiology*, 110:905–909, 1999.
- [6] E. Kaukoranta, M. Hämäläinen, J. Sarvas, and R. Hari. Mixed and sensory nerve stimulations activate different cytoarchitectonic areas in the human primary somatosensory cortex SI. *Exp. Brain Res.*, 63(1):60–66, 1986.
- [7] R. Vigário, J. Särelä, V. Jousmäki, M. Hämäläinen, and E. Oja. Independent component approach to the analysis of EEG and MEG recordings. *IEEE Trans. Biomed. Eng.*, 47:589–593, 2000.
- [8] R. Vigário, J. Särelä, V. Jousmäki, and E. Oja. Independent component analysis in decomposition of auditory and somatosensory evoked fields. In *Proc. Int. Workshop on Independent Component Analysis and Blind Separation of Signals (ICA '99)*, Aussois, France, 1999.
- [9] R. Vigário, J. Särelä, and E. Oja. Independent component analysis in wave decomposition of auditory evoked fields. In *Proc. Int. Conf. on Artificial Neural Networks (ICANN'98)*, Skövde, Sweden, 1998.